01,07

Analysis of Al nanocrystals nucleation in $Al_{87}Ni_8Y_5$ metallic glass under constant heating rate conditions

© S.V. Vasiliev[1,2], E.A. Sviridova[1,2], V.I. Tkatch[1]

[1] Galkin Donetsk Institute for Physics and Engineering, Donetsk, Russia
[2] Donbass National Academy of Civil Engineering and Architecture, Makeyevka, Russia

E-mail: ksvir@list.ru

Received March 11, 2024
Revised March 26, 2024 Accepted March 27, 2024

The process of formation of a nanocomposite amorphous-nanocrystalline structure in $Al_{87}Ni_8Y_5$ metallic glass under heating with rate of 0.083 K/s was investigated by differential scanning calorimetry, electrical resistance measurements and X-ray diffraction. Taking into account the features of the nanocomposite structure, the model for nucleation rate changes $J(T)$ determination using the experimentally estimated changes of size and volume fraction of nanocrystals was proposed. The dependence of $J(T)$, obtained in this way, was analyzed in the frames of the classical equation of temperature dependence of homogeneous nucleation rate. The numerical values of the parameters in this equation, resulting for the best agreement with the experiment, were determined, and possible reasons of discrepancies were discussed.

Keywords: metallic glass, nanocomposite structure, model, size and volume fraction of nanocrystals, classical equation of homogeneous nucleation.

DOI: 10.61011/PSS.2024.07.58980.50

1. Introduction

Due to their outstanding strength (up to 1.5 GPa), the amorphous-nanocrystalline (nanocomposite) structures in aluminium alloys (with aluminium content of 80−90 at.%), alloyed with rare-earth and transition metals [1], attract much interest of the researchers to this class of metallic materials. The nanocomposite structures are formed during the process of partial (nano-) crystallization of amorphous phases in Al-based alloys obtained by melt quenching, and consist of nanocrystals of pure aluminium with typical sizes 10−30 nm and volume density of $10^{21}-10^{23}$ m^{-3}, distributed within the residual (70−80%) amorphous matrix enriched with alloying elements. The strength properties of solids materials are structure-sensitive, therefore, conditions and trends of the nano-phase composites formation were extensively studied since the moment when such structures had been first synthesized [2,3].

According to a widely used classification of the processes of metallic glasses transition into crystalline state [4], that of formation of crystals with composition different from the parent phase is called primary crystallization which, by its nature, is generally the first transformation stage. It's obvious that crystallite sizes and their volume density in the crystallized glasses are determined by the ratio of rates of the two crystallization components — processes of crystals nucleation J and growth U, and, consequently, the formation of nano-scale structures is possible only with a combination of high J and low U values. The theoretical analysis in paper [5] on the growth of primary Al nanocrystals, demonstrated that the rate of this process is reduced due to formation of shells (diffusion zones) around the growing crystallites; these shells are enriched with atoms of rare-earth and transition metals insoluble in solid aluminium. The diffusion zones retard the fluxes of Al atoms going towards the surface of growing nanocrystals, while impingement of zones of the neighboring crystallites results in the full stop of their growth. The existence of diffusion zones was confirmed experimentally [6], while the subsequent studies confirmed the correctness of „soft" impingement model [7], which served the basis for development of the approximate analytical approaches describing the growth of nanocrystals in isothermal conditions [8] and during heating with a constant rate [9].

In contrast to growth, the mechanisms of crystals nucleation in the nano-composite structures so far have still been discussed. According to some authors [10,11], the classical theory of stationary homogenous nucleation cannot explain high density of nanocrystals, since it predicts the low rates at temperatures close to the glass transition temperature. Therefore, to explain the high density of nanocrystals the models based on heterogeneous nature of the amorphous structure formed during solidification or on the structural relaxation process were considered. As such heterogeneous inclusions the quenched-in nuclei of Al [5] or concentration inhomogeneities (clusters enriched with Al) formed during phase separation [12] or solidification [13] have been considered. In fact, the quenched-in nuclei and signs of phase separation were observed experimentally in some Al-based glasses [13,14], however, these structural features are not necessary condition for the formation of

high-density nanocrystals. Yet, according to authors of [15], the presence of concentration inhomogeneities is necessary for the formation of nano-composite structures, and on this base a quantitative model has been offered recently, describing the process of Al nucleation in amorphous alloy $Al_{88}Y_7Fe_5$ [16]. The nucleation rate equation used in the model formally coincides with the classic equation, however it is based on experimentally defined density $5.2 \cdot 10^{25}\,m^{-3}$ of Al-enriched 1.7 nm diameter areas for this glass. Despite good coincidence of the analytical data and experimental estimates, the complicated nature of the model and presence of large number of parameters make its use limited in the analysis of other glasses' nano-crystallization processes.

On the other hand, the quantitative analysis in paper [17] for the changes in Al nanocrystals nucleation rate during heating of metallic glass $Al_{87}Ni_8Y_5$ with a rate of 0.083 K/s demonstrated the possibility in principle to describe this process within the frames of classical homogenous nucleation theory. However, this result was obtained using a number of approximations: (i) the kinetics of the crystallized volume fraction variation was determined based on changes of electrical resistance; (ii) in determination of nanocrystals sizes from the width of diffraction maxima the instrumental broadening was neglected; (iii) in the equation for estimation the nucleation rate from the ratio between the variation rate of the crystallized volume fraction and nanocrystals sizes the value of the transformed fraction was neglected; (iv) the specific free energy of the nucleus/amorphous phase interface was taken temperature independent; (v) the effective diffusivity was determined from the results of isothermal studies. Accounting this circumstance, it was found reasonable to make a more rigorous analysis of the process of nanocrystals nucleation in glass $Al_{87}Ni_8Y_5$ using the results of differential scanning calorimetry and the modified models, which was the purpose of this study.

2. Model

As mentioned above the process of nano-crystallization occurs by way of crystals nucleation and subsequent diffusion-controlled growth, the rate of which decreases down to zero due to impingement of diffusion fields around each growing crystallite, but not due to impingement of the crystallites themselves which are mainly spherical in shape. In case of an isothermal process the function of crystals size distribution L may be given as:

$$N(t, L) = N_0(t)n(t, L), \tag{1}$$

where t is time, $N_0(t)$ is crystals volume density, $n(t, L)$ is the normalized function of their size distribution,

$$\int_0^\infty n(t, L)dL = 1.$$

If spherical shape of growing nanocrystals is assumed, the change of the crystallized volume fraction $X(t)$ can be described by the relation

$$X(t) = \frac{\pi}{6}\int_0^\infty N(t, L)L^3 dL = \frac{\pi}{6}N_0(t)\int_0^\infty n(t, L)L^3 dL, \tag{2}$$

from which the crystals density $N_0(t)$ may be expressed as follows:

$$N_0(t) = \frac{X(t)}{\frac{\pi}{6}\int_0^\infty n(t, L)L^3 dL}. \tag{3}$$

On the other hand, the crystals density $N_0(t)$ may be expressed via the nucleation rate $J(t)$:

$$N_0(t) = \int_0^t J(t')\big(1 - X(t')\big)dt'. \tag{4}$$

By equating the relations (3) and (4) and differentiating the obtained equality with respect to time we may find the expression for the nucleation rate in isothermal conditions as:

$$J(t) = \frac{1}{1 - X(t)}\frac{\pi}{6}\frac{d}{dt}\left(\frac{X(t)}{\int_0^\infty n(t, L)L^3 dL}\right). \tag{5}$$

Accounting that

$$\frac{\pi}{6}\int_0^\infty n(t, L)L^3 dL$$

is by definition an average volume of particle $\langle V\rangle$, the change of nucleation rate in the isothermal conditions (5) will be written as

$$J(t) = \frac{1}{1 - X(t)}\frac{d}{dt}\left(\frac{X(t)}{\langle V(t)\rangle}\right) = \frac{1}{1 - X(t)}\frac{6}{\pi}\frac{d}{dt}\left(\frac{X(t)}{\langle L^3(t)\rangle}\right), \tag{6}$$

and for heating with constant rate q $(dt = dT/q)$

$$J(T) = \frac{q}{1-X(T)}\frac{d}{dT}\left(\frac{X(T)}{\langle V(T)\rangle}\right) = \frac{q}{1-X(T)}\frac{6}{\pi}\frac{d}{dT}\left(\frac{X(T)}{\langle L^3(T)\rangle}\right). \tag{7}$$

If we suggest [18,19], that nano-crystallization process is controlled by nucleation (the model of „instantaneous growth"), then, the function of size distribution$(n(t, L))$ can be represented as $n(t, L) = \delta(L - L_{fin})$, where $\delta(x)$ is Dirac delta function, and L_{fin} is final size of nanocrystal. By substituting this expression in (5), we obtain expressions (8) and (9) for the isothermal and non-isothermal processes, respectively.

$$J_{inst}(t) = \frac{6}{\pi}\frac{1}{L_{fin}^3[1 - X(t)]}\frac{dX}{dt}, \tag{8}$$

$$J_{inst}(T) = \frac{6}{\pi} \frac{q}{L_{fin}^3[1 - X(T)]} \frac{dX}{dT}. \quad (9)$$

It should be noted, that electron-microscopic studies of the structure of nano-phase composites formed during the first stage of Al-based glass crystallization, showed that [15,19–21], despite high volume density of nanocrystals no direct contact between them was observed such lending support to the suggested model.

As follows from equations (6) and (7), to determine the variation of the nucleation rate during nano-crystallization process within the proposed model we need to have experimentally found dependencies of the fraction of crystallized volume and nanocrystals sizes depending on the time of exposure or heating temperature. To exclude any uncertainties that may arise from the heating-up times in the course of isothermal studies, and for comparison with the results of the above-mentioned analysis [17] this paper considers the process of nano-crystallization of $Al_{87}Ni_8Y_5$ glass during heating with a rate of 0.083 K/s.

3. Materials and research techniques

Metallic glass with the nominal composition of $Al_{87}Ni_8Y_5$ was produced as a ribbon 10 mm wide and $50 \pm 3\,\mu$m thick by ejecting of the melt onto a rotating copper wheel in a helium atmosphere. The structural parameters of nano-composites formed in the thermally treated samples were determined from the diffraction patterns obtained by an automated standard diffractometer DRON-3M using filtered Co K_α-radiation. The volume fraction crystallized was determined from the ratio of total area of diffraction maxima (111) and (200), A_{cr}, to the intensity of scattered radiation in the range of diffused halo angles ($2\theta = 30{-}65°$) [22,23]: $X = A_{cr}/(A_{cr} + A_{am})$, where A_{am} is the integral intensity of halo. Average sizes of Al nanocrystals were calculated from the Selyakov–Sherrer relation [24] $L = \lambda/(B_{111}\cos\theta_{111})$, where λ is the wavelength of the radiation, B_{111} is the integral width of reflection (111) accounting instrumental broadening, and θ_{111} is the diffraction angle. The volume density of nanocrystals was assessed as $N = 6X/(\pi L^3)$.

The samples were thermally treated by heating with a rate of 0.083 K/s. The kinetics of crystalline phases formation was evaluated from the thermograms measured by differential scanning calorimetry (DSC) (NETZSCH DSC 404 calorimeter) and from the variations of electrical resistance (four-probe potentiometric method). Kinetic curves of nano-crystallization $X(T)$ were plotted based on the variations of heat flow and relative electrical resistance (ER) normalized to the fraction of crystallized volume determined by X-ray method in the sample heated to a temperature when the first crystallization stage is completed. The variations of nanocrystals sizes during heating were determined by X-ray method on the rapidly cooled samples (with a rate of 4 K/s) down from different temperatures within the nanocrystallization range.

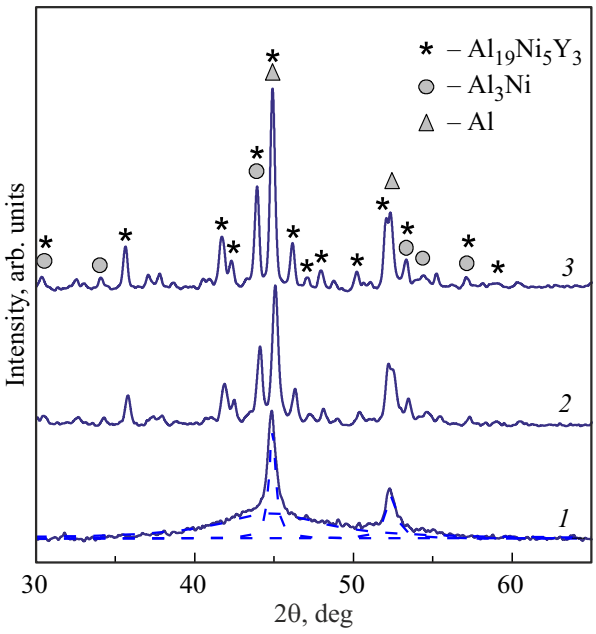

Figure 1. The diffraction patterns of the rapidly cooled ribbon $Al_{87}Ni_8Y_5$ after heating with a rate of 0.083 K/s to temperatures 553 (*1*), 602 (*2*) and 620 (*3*) K. The dashed lines show the contributions of amorphous matrix and Al nanocrystals to the diffraction pattern of a nano-composite structure (*1*).

4. Results

Amorphous nature of the rapidly cooled alloy ribbon $Al_{87}Ni_8Y_5$, studied in this paper, is confirmed by the results of X-ray studies (Figure 1). From data shown in Figure 1 it follows that transition of the amorphous structure into crystalline state occurs through the three sequential exothermic reactions, where each reaction is accompanied by a drop of electrical resistance. The X-ray analysis of the samples subjected to heating with a rate of 0.083 K/s to temperatures 553, 602 and 620 K, corresponding to completion of each transformation stage, shows that (Figure 1) during the first stage of crystallization in the amorphous matrix the nanocrystals of pure Al are formed, during the second stage the residual amorphous matrix is crystallized with formation of crystals Al_3Ni and $Al_{19}Ni_5Y_3$ and growth of primary Al nanocrystals, and the third maximum of heat output occurs due to coarsening of the structural components.

From comparison the results of the DSC and resistometric studies (Figure 2) it follows that, temperatures of the rate transformation maxima at each stage practically coincide (scatter doesn't exceed 1 K), while the profile shapes slightly differ. In particular, the analysis of the nanocrystallization rate profiles (the inset in Figure 2) shows that temperatures of DSC curves extremes and ER derivatives are 494.5 and 493.8 K respectively, while the temperature of crystallization onset (the point of intersection of the baseline and the tangent at the inflection point) of DSC curve (478.1 K) is approximately by 1 K lower, than that

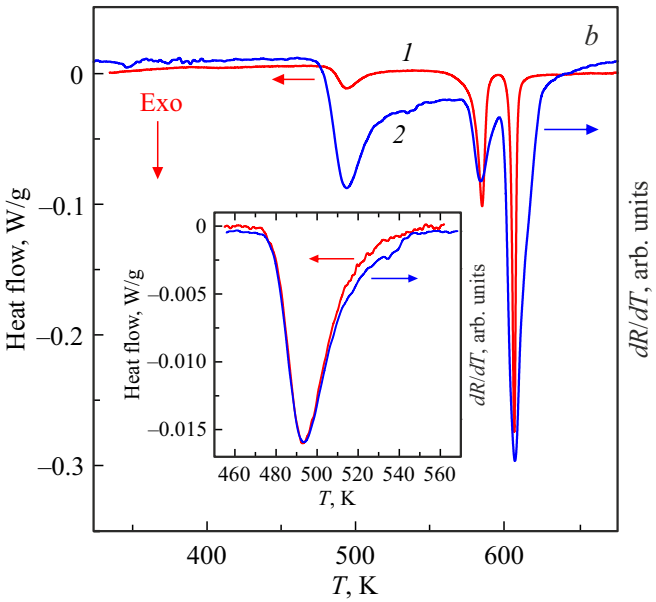

Figure 2. DSC thermogram (*1*) and changes of ER derivative (*2*) of amorphous $Al_{87}Ni_8Y_5$ ribbon during heating with a rate of 0.083 K/s in the temperature range of complete transition into crystallite state; inset — illustrates the fragments of the curves in the range of nanocrystallization temperatures.

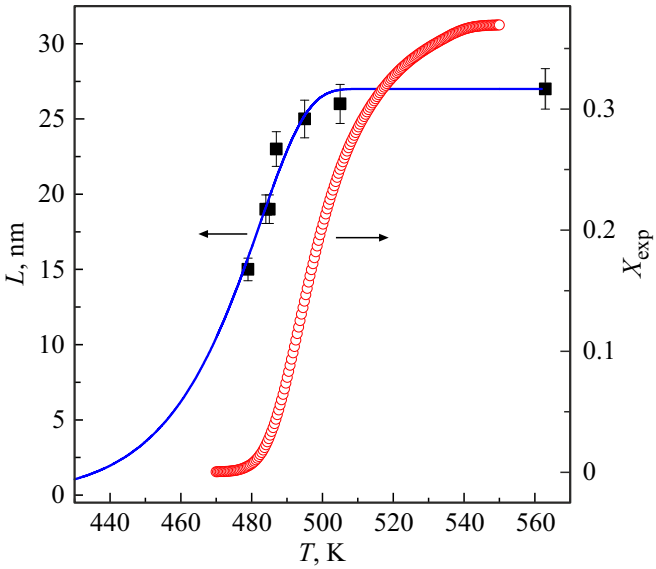

Figure 3. Variation of average size of the nanocrystals and fraction of crystallized volume in metallic glass $Al_{87}Ni_8Y_5$ during heating with a rate of 0.083 K/s.

according to ER data (479 K). Similar agreement between the DSC and resistometric study results was observed also for the amorphous alloy $Al_{85}Ni_5Y_8Co_2$ [25], indicating the possibility of using the ER measurement method for analysis of nanocrystallization process kinetics. However, in view that variations in the heat flux are strictly proportional to the change of the crystallized volume fraction the DSC data were used in the subsequent analysis in this paper.

The integration of DSC thermogram, shown in Figure 2, and normalization of the obtained curve to the value of $X = 0.37$, determined from the diffraction pattern of the sample heated up to 553 K, gives the nanocrystallization kinetic curve $X(T)$, shown in Figure 3, which tends to saturation at temperatures above 540 K. In contrast to $X(T)$, the nanocrystals sizes show the „plateau“ ($L = 27 \pm 1$ nm) at much lower temperature (~ 500 K), Figure 3. From combination of the determined parameters of the nanocomposite structure it follows that volume density of Al crystals is $3.6 \cdot 10^{22}\,\mathrm{m}^{-3}$, which is typical for the Al-base nanophase composites [5,20].

5. Analysis and discussion determined

As follows from equation (7), the nucleation rate changes versus temperature during nanocrystallization $J(T)$ are defined by the ratio between kinetics of increase of the crystallized volume fraction $X(T)$ and nanocrystals sizes $L(T)$, shown in Figure 3. However, due to a limited number of the experimentally determined values of grain sizes the operation of numerical differentiation is not correct. For this reason the values of $L(T)$, shown by points in Figure 3, were approximated by the relation [9]

$$L(T) \approx \sqrt{8/3}/\lambda_H r_S \left[1 - \exp\left(-3\lambda_H D(T) t_{\mathrm{eff}}(T)/r_S^2\right)\right]^{1/2}, \quad (10)$$

which described the growth of nanocrystals under conditions of diffusion fields impingement during heating at constant rate. Here r_S is the half-distance between Al nanocrystals at the final stage of nanocrystallization, $D(T) = D_0 \exp(-Q_D/T)$ is the diffusion coefficient governing transition of Al atoms from amorphous matrix to nanocrystal, $t_{\mathrm{eff}} = T^2/(qQ_D)$ is the effective time of non-isothermic process with activation energy Q_D, $\lambda_H = [(C_\mathrm{I} - C_\mathrm{M})/(C_\mathrm{I} - C_\mathrm{P})]^{1/3}$ is the parameter depending on concentration of alloying elements in the matrix, C_M, crystal, C_P, and at the interface between them, C_I. Assuming that $C_\mathrm{I} = 2C_\mathrm{M} - C_\mathrm{P}$ [9], and taking into account that concentration of alloying elements in the alloy $Al_{87}Ni_8Y_5$ is 0.13, and nanocrystals do not contain the alloying elements, the value of parameter λ was taken to be 0.794.

In paper [17] cited above, in equation (10) the values of $D(T)$ estimated from the changes of $L(t)$ during isothermal annealings. However, the values $L(t)$, that were used for these estimates, calculated neglecting the correction for instrumental broadening, were significantly lower ($L_{fin} = 17.5$ nm) than the values shown in Figure 3. Therefore, we determined the parameters of equation (10) $D(T)$ and r_S by matching the analyzed curve and experimentally found values. The matching procedure was highly sensitive to selection of the fitting parameters, and the curve in Figure 3 with the value of reduced $R^2 = 0.973$ was obtained with the use of the following values: $D_0 = 240.2\,\mathrm{m}^2/\mathrm{s}$, $Q_D = 22702$ K, $r_S = 20.82$ nm.

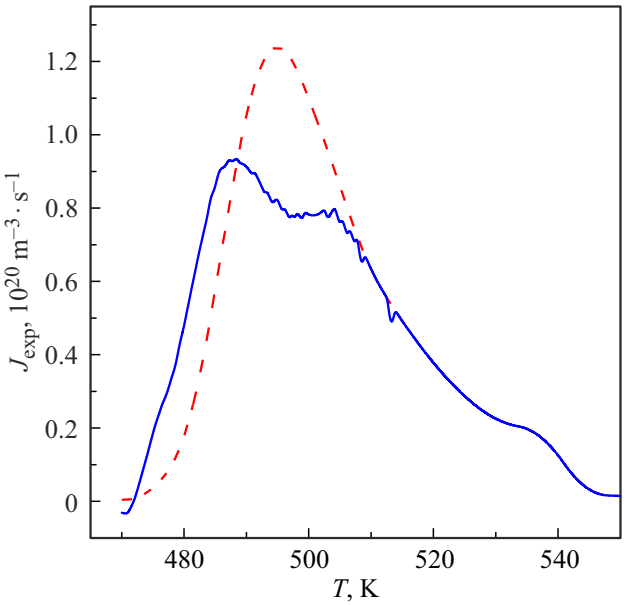

Figure 4. The rate of Al nanocrystals nucleation variation in glass $Al_{87}Ni_8Y_5$, calculated accounting the variations of nanocrystal sizes (solid line, equation (7)) and under assumption of instantaneous growth (dash line, equation (9)).

By substituting the experimentally found dependence of $X(T)$ and the calculated dependence of $L(T)$ into equation (7) we obtain the Al nanocrystals nucleation rate versus temperature during heating with a rate of 0.083 K/s, shown by the solid line in Figure 4. As seen from the analysis, the nucleation rate as a function of temperature has a maximum ($9.4 \cdot 10^{19}$ m$^{-3}\cdot$s^{-1} at a temperature of 488.5 K) with an „arm“ at temperature of about 503 K. The curve $J_{inst}(T)$ calculated within the instantaneous growth model (equation (9)) has a more simple shape (Figure 4). This is not surprising, since the shape of this curve having maximum $1.24 \cdot 10^{20}$ m$^{-3}\cdot$s^{-1} at 494.5 K, as follows from equation (9), is close to the heat flow curve on DSC thermogram.

In view that, according to the classic theory, the temperature dependence of the homogeneous nucleation rate is the curve with a maximum, it was interesting to compare the theoretical curves with those shown in Figure 4 and to analyze, if it is possible to use the classical nucleation theory (CNT) to describe the formation of experimentally found high density of nanocrystals.

As well known [26], main principles of CNT developed in the middle of past century for small equilibrium deviations are based on several assumptions, among which the major ones are zero thickness of nucleus-to-parent phase interface (Gibbs capillary approximation) and applicability of macroscopic parameters for characterization of nanoscale nuclei. However, the theoretical analysis and experimental studies carried out in the second half of XX century, demonstrated that the modified versions of CNT are applicable for description of the nucleation processes in the highly non-equilibrium systems (in glasses [27]), under non-isothermic [28] and nonstationary conditions [29]. Subsequent studies allowed to establish the time stages of the nucleation process [30–32], as well as to take into account the finite thickness of interface [33], curvature of nucleus surface [34,35], the influence of mechanical and chemical factors [36] and a multi-component nature of systems and possibility of nucleation of various phases [31]. However, the above-mentioned and some other modifications of the theoretical nucleation model [37] include additional (often, not a priori) parameters, the estimation of which in experimental conditions is somewhat complicated.

Taking into account these circumstances, in this study we made an attempt to carry out an approximation analysis of $J(T)$ curves, determined from experimental data (Figure 4), within the most simple equation of the steady state rate homogenous nucleation within the Turnbull–Fisher model [38] as

$$J_{st}(T) = \frac{N_V D_0}{a_0^2} \exp\left(-\frac{Q_D}{T}\right) \exp\left[-\frac{16\pi\sigma(T)^3 V_m^2}{3kT\Delta G(T)^2}\right] = J_0 \exp\left[-\frac{Q_D + W(T)}{T}\right], \quad (11)$$

where N_V is the number of atoms per unit volume, a_0 is the length of diffusion jump through the interface (taken equal to the average atomic diameter), $\Delta G(T)$ is the thermodynamic driving force, $\sigma(T)$ is the specific free energy of nucleus/matrix interface, $W(T)$ is the work of formation of a critical size nucleus, V_m is the molar volume, k is the Boltzmann constant.

Equation (11) has a number of constants and temperature-dependent parameters. Since nucleation of pure Al crystals is analyzed, the values of $N_V = 6.02 \cdot 10^{28}$ m^{-3}, $a_0 = 2.86 \cdot 10^{-10}$ m and $V_m = 1.06 \cdot 10^{-5}$ m^3 for this element were taken from the reference literature [39]. The change in the Gibbs thermodynamic potentials difference for liquid and crystalline phases $\Delta G(T)$ can be calculated if we know the temperature dependencies of their heat capacity. However, because of the practically full absence of such data for the glass forming alloys, to calculate the changes $\Delta G(T)$ a number of the approximate models is used [27]. For this purpose, in this paper we used the Thompson–Spaepen model [40]:

$$\Delta G(T) = \frac{2\Delta H_m T(T_m - T)}{T_m(T_m + T)}, \quad (12)$$

where ΔH_m and T_m are latent heat and melting temperature, respectively, taken for pure Al as 10784 J/mol and 933.5 K [39]. As it was established in a number of studies (e.g., [41]), this simple model quite correctly described the difference of the thermodynamic potentials for many glass forming alloys and due to this fact this model became widely applied.

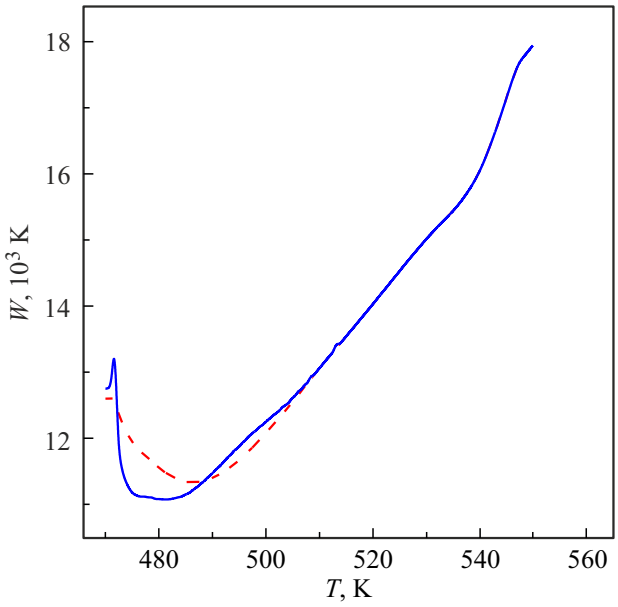

Figure 5. The changes of the work of critical nucleus size formation in glass $Al_{87}Ni_8Y_5$ at heating with a rate of 0.083 K/s, calculated accounting the variations of nanocrystal sizes (solid line) and for instantaneous growth case (dash line).

If, in accordance to the classical crystallization theory, we assume that crystals nucleation and growth processes have the same diffusion nature [26], then, in equation (11) the only temperature dependence of the specific free energy of the nucleus/matrix interface $\sigma(T)$ remains unknown. As it follows from equation (11), the nucleation rate significantly depends on the value of σ, while the existing structural and thermodynamic models (e.g., [42,43]) do not provide the needed accuracy for analysis of specific metals and alloys. For this reason, the variation $\sigma(T)$ was taken as a model parameter and was determined by comparison with experimental data. In this study, the dependence of $\sigma(T)$ was calculated from changes of the work of the critical nucleus formation which calculated from the expression

$$W(T) = -T \ln\left[\frac{J_{\exp}(T)}{J_0 \exp(-Q_D/T)}\right], \qquad (13)$$

which for the values $J_{\exp}$ found from the models (7) and (9) (Figure 4) is shown in Figure 5.

As seen from Figure 5, with the temperature increase the work of critical nucleus formation within the nanocrystallization temperature range changes by non-monotonic way, which contradicts the classical theory which predicts that W must monotonously grow with approaching the melting temperature. It should be noted that the similar abnormal behavior of $W(T)$ was observed during crystallization analysis of a number of oxide glasses [44]. According to authors of this paper, the enhanced values of W at temperatures below the maximum of nucleation rate are explained by relaxation processes in glasses which are neglected in the crystallization theory. By comparing the dependencies of $J(T)$ shown in Figure 4, and $W(T)$ in Figure 5 we may see that at temperatures above those corresponding to $J_{\max}$ (488.5 and 494.5 K) the values of nucleation work grow monotonously with the temperature rise. Apparently the similar behavior of the $W(T)$ curves at initial crystallization stages of $Al_{87}Ni_8Y_5$ metallic glass and the oxide glasses indicates that the observed variations have the same nature which clarification requires additional research.

For this reason, to calculate the temperature dependencies of the specific free interfacial energy $\sigma(T)$ using the relation

$$\sigma(T) = \left[\frac{3kW(T)\Delta G(T)^2}{16\pi V_m^2}\right]^{1/3} \qquad (14)$$

the values of $W(T)$ at temperatures above 490 K were used in combination with dependence $\Delta G(T)$, calculated using equation (12) (curve *1* in Figure 6). As seen from Figure 7, the values of σ grow with the increase of temperature which is consistent with the classical crystallization theory [42], and they are well approximated by the linear dependence $\sigma(T) = 0.026 + 1.55 \cdot 10^{-4}T$. This relation describes $\sigma(T)$, calculated based on the nucleation work variation which takes into account the growth of nanocrystals. Substituting into (14) the values of $W(T)$ calculated in the instantaneous growth model (dash line in Figure 5), yields the close values of σ_i (not shown in the Figure), approximated by the relation $\sigma_i(T) = 0.02 + 1.66 \cdot 10^{-4}T$. The values σ obtained from these relations within the nanocrystallization temperature range (480–520 K) lie within 0.1–0.106 J/m^2, which is somewhat higher than the estimates (0.07 and 0.076 J/m^2) of the specific free energy of nucleus interface governing formation of nanocrystals in $Al_{88}Y_7Fe_5$ [45] and $Al_{88}Y_8Ni_4$ [46] glasses, respectively. The

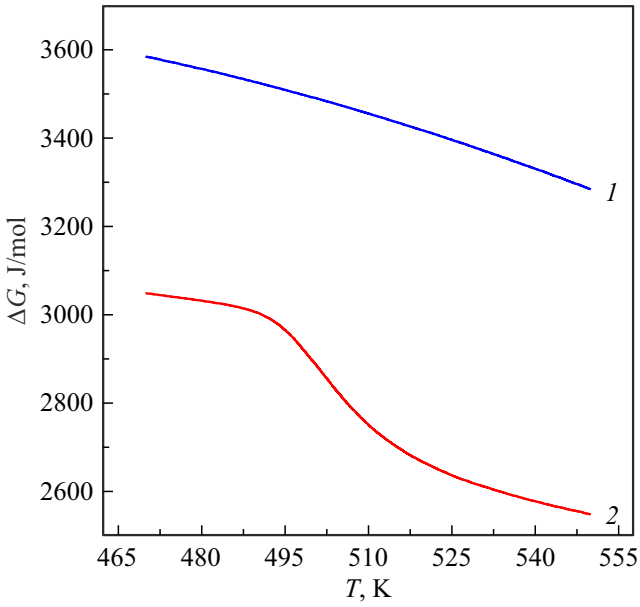

Figure 6. Temperature dependencies of thermodynamic potentials difference between $Al_{87}Ni_8Y_5$ melt and crystalline Al, calculated from the expressions (12) — (*1*) and (15) — (*2*).

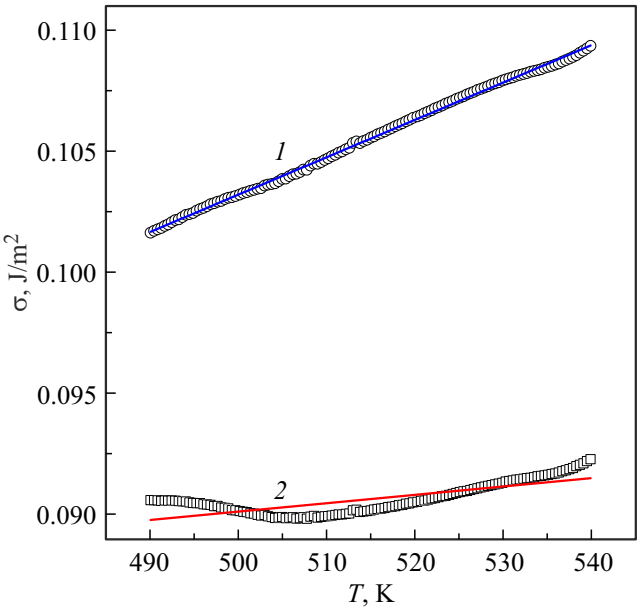

Figure 7. Temperature dependencies of the specific free energy of nucleus/amorphous phase interface calculated neglecting (*1*) and taking into account (*2*) the variations in parent phase composition.

extrapolation of the above-mentioned linear dependencies to the melting temperature of Al (933.5 K) also yields the enhanced values of σ (0.175 and 0.171 J/m^2 respectively), compared to the specific free energy of Al nucleus interface in its own melt equal 0.108 J/m^2 [27].

Equation (12) used in $\sigma(T)$ analysis describing the variation of the thermodynamic driving force was obtained under assumption that the nucleus and parent phase had identical composition. However, nanocrystallization of amorphous alloy $Al_{87}Ni_8Y_5$ occurs through formation of pure Al nucleus in the matrix containing 13 at.% of alloying elements (C_{M0}), and as the crystallized volume fraction X increases the concentration of matrix, C_M, continuously grows according to law $C_M(X) = C_{M0}/(1-X)$. It is evident that the thermodynamic stimulus for the formation of nucleus having composition different from the parent phase, will be lower than that of the nucleus with identical composition, and the difference in driving force will grow with the increase of the difference in compositions. Analysis of the change in thermodynamic driving force for the pure component nucleus formation caused by the matrix composition variation, performed within the regular solutions model [47] allowed to obtain the following expression:

$$\Delta G_{ex}(C_M, T) = (T_m - T)\{\Delta S(T) + R\ln[1 - C_M(X)]\}, \quad (15)$$

where R is the universal gas constant, and $\Delta S(T) = 2\Delta H_m T/[T_m(T_m + T)]$. The calculations showed that (curve *2* in Figure 6) if we take into account the difference in compositions of nucleus and matrix the difference of the thermodynamic potentials is reduced by about 500 J/mol (15%) at initial nanocrystallization stages and approximately by 750 J/mol (23%) in the end. Since $W(T)$ in expression (14) remains the same, then, reduction of ΔG, correspondingly, results in the lower interfacial specific free energy values which in the range of the nano-crystallization temperatures lie in the range of 0.089–0.091 J/m^2 (Figure 7, curve *2*). The temperature dependencies of σ calculated using ΔG_{cx}, both, accounting the changes in the nanocrystals sizes, and in the instantaneous growth model, are approximated by the linear functions $\sigma_{cx}(T) = 0.073 + 3.46 \cdot 10^{-5}T$ and $\sigma_{cxi}(T) = 0.067 + 4.51 \cdot 10^{-5}T$, and their values at Al melting temperature are 0.105 and 0.109 J/m^2, respectively.

The estimated variations of $\sigma(T)$ (Figure 7) and corresponding calculated temperature dependence of thermodynamic driving force (Figure 6) allows to determine the variation of radius of Al critical nucleus as $r_{cr} = 2\sigma V_m/\Delta G$ [26]. The calculations showed that for a combination of $\sigma(T)$ with$\Delta G(T)$, obtained from equation (12), (the curves *1* in Figures 6 and 7), the radii of critical nucleus in glass $Al_{87}Ni_8Y_5$ within the range of nanocrystallization temperatures (470–530 K) increased from 0.58 to 0.72 nm, and for the combination of curves *2* grew from 0.62 to 0.76 nm. The obtained results seem reasonable, because they are close to the experimental estimate $r_{cr} = 0.85$ nm of Al nucleus in metallic glass $Al_{88}Y_7Fe_5$ [16].

By substituting the obtained dependencies $\sigma(T)$ in equation (11) we may calculate the temperature dependencies of homogenous nucleation rates within the nanocrystallization temperatures range. By comparing the curves $J(T)$ calculated in the models accounting the growth of nanocrystals (Figure 8, *a*) and for instantaneous growth (Figure 8, *b*) with the appropriate curves calculated from the experimental data, (Figure 4) we see that using the combination of dependencies of $\sigma(T)$ and $\Delta G(T)$ (curves *1* in Figures 6 and 7), yields the very wide curves compared to the experimental ones which have the high values at temperatures below the crystallization onset temperatures. The temperature ranges of $J(T)$ changes calculated using the $\Delta G_{cx}(T)$ dependence, are in better agreement with the curves $J(T)$, determined from the experimental data (curves *2* and *3* in Figure 8). As can be seen from Figure 8, *a*, the temperatures of maxima at curves $J(T)$, determined taking into account the finite growth rate, coincide (487 K), however, the calculated value J_{max} ($1.3 \cdot 10^{20}$ m$^{-3} \cdot$ s^{-1}) is about 1.4 times higher than J_{exp} ($0.93 \cdot 10^{20}$ m$^{-3} \cdot$ s^{-1}). In contrast to these data, the temperatures of maxima of the calculated and experimental dependencies $J(T)$, found from the instantaneous growth model, are different (486 and 495 K respectively), and the values of J_{max} ($2.6 \cdot 10^{20}$ and $1.24 \cdot 10^{20}$ m$^{-3} \cdot$ s^{-1}) differ more than twice (Figure 8, *b*).

Based on the results in Figure 8, we can say that temperature dependencies of Al nanocrystals nucleation rates, within the model of classical homogenous nucleation with the correct values of the specific free interfacial energy, are in reasonable agreement with the curves

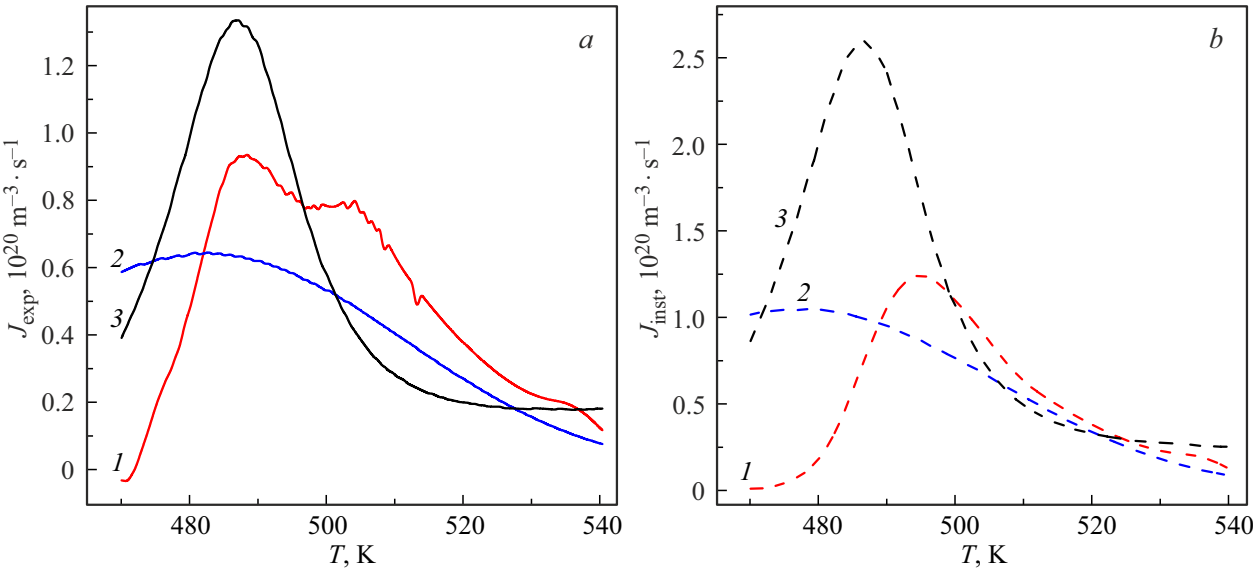

Figure 8. Variations of homogenous nucleation rates during nanocrystallization of $Al_{87}Ni_8Y_5$ glass, determined and calculated accounting the nanocrystals growth (a) and in the model of instantaneous growth (b): *1* — $J_{exp}(T)$, *2* — calculated for combination of $\Delta G(T)$ and $\sigma(T)$, *3* — calculated from the combination of $\Delta G_{cx}(T)$ and $\sigma_{cx}(T)$.

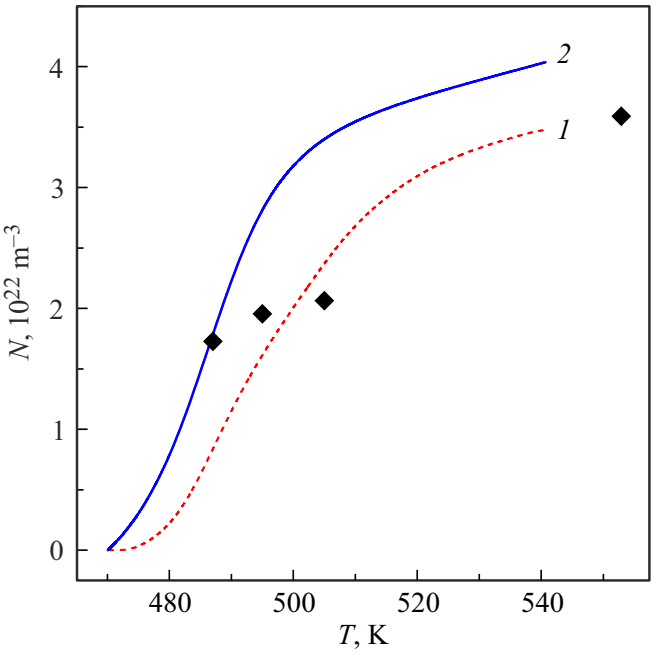

Figure 9. Variations of Al nanocrystals volume density during nanocrystallization of metallic glass $Al_{87}Ni_8Y_5$ at heating with a rate of 0.083 K/s: *1* — integration of $J_{exp}(T)$, *2* — integration of calculated dependence $J(T)$, the symbols are estimates based on the X-ray determined values of X and L.

$J_{exp}(T)$ characterizing the changes in nucleation rate during nanocrystallization. As additional verification of a possibility to describe the formation of the high density of nuclei with equation (11) with the use of $J(T)$ dependence obtained taking into account the variation of nanocrystals sizes (curve *3* in Figure 8, a), we have calculated the variation in density of nuclei $N(T)$ during nanocrystallization process as

$$N(T) = q^{-1} \int_{T_1}^{T} J(T')[1 - X(T')]dT'.$$

Integration within the temperature range of 470–540 K showed that the calculated values of N had good correlation with the Al nanocrystal density determined from the XRD studies (Figure 9), though the final value ($4.04 \cdot 10^{22}$ m^{-3}) was slightly higher than the experimental one ($3.6 \cdot 10^{22}$ m^{-3}). It is not surprising, since the calculated nucleation rates within the temperature range below the temperature of maximum are significantly higher than the experimental ones.

One of the probable reasons of the observed difference in curves $J(T)$ shape is the non-stationary behavior of nucleation process which is typical for many metallic glasses [16,48], which is neglected in equation (11). To take into account the influence of non-stationary behavior on the nucleation rate it is necessary to include into equation (11) the multiplier describing the temperature dependence of the characteristic transient time which can be determined by additional experiments in isothermal conditions [16,48].

6. Conclusions

The results of the experimental studies of non-isothermic nanocrystallization kinetics, structural changes in metallic glass $Al_{87}Ni_8Y_5$ and their analysis allow to draw the following conclusions:

1. According to the practically identical results, obtained by DSC and measurements of electrical resistance, the first

crystallization stage at heating with a rate of 0.083 K/s starts at a temperature of 479 K and takes place up to 540 K by formation in the amorphous matrix the nanocrystals of pure Al, the volume fraction of which and sizes are 0.37 and 27 nm respectively.

2. Accounting the features of the nano-phase composites structure (absence of nanocrystals impingement) the model was proposed for estimation of the nucleation rate variations during heating by measuring the sizes of nanocrystals $L(T)$ and their volume fraction $X(T)$, as well as by the assumption of instantaneous growth.

3. It was found that experimentally measured values of $L(T)$ are correctly approximated through the approximate equation of diffusion-controlled growth, that allowed to establish the temperature dependence of the diffusion coefficient controlling the growth of nanocrystals.

4. The dependencies of $J_{\exp}(T)$ calculated based on experimental data within the nucleation rate model showed the maxima of $9.3 \cdot 10^{19}\,\mathrm{m}^{-3} \cdot \mathrm{s}^{-1}$ at 487 K and $1.24 \cdot 10^{20}\,\mathrm{m}^{-3} \cdot \mathrm{s}^{-1}$ at 495 K for the cases of nanocrystals sizes variation and of instantaneous growth, respectively.

5. The analysis of dependencies $J_{\exp}(T)$ within the equation of homogenous nucleation classical theory showed that the most close to the experiment was the dependence $J(T)$ ($J_{\max} = 1.33 \cdot 10^{20}\,\mathrm{m}^{-3} \cdot \mathrm{s}^{-1}$ at 487 K), calculated using the Thompson–Spaepen model which described the temperature dependence of the thermodynamic driving force in a variable concentration matrix.

6. The correctness of the performed analysis is proved by good consistency with the literature data on specific interfacial free energy values, which in the range of nanocrystallization temperatures lie within $0.089-0.091\,\mathrm{J/m}^2$, and by the reasonable estimates of sizes of critical nuclei.

7. The higher values of the calculated $J(T)$ curves compared to the values determined from the experimental data at the area of temperatures below maximum, are probably explained by a non-stationary behavior of the nucleation process which is neglected in the used homogenous nucleation model. The transient behavior of nucleation results in lower volume density of nanocrystals ($3.6 \cdot 10^{22}\,\mathrm{m}^{-3}$), determined experimentally, compared to the calculated density ($4.04 \cdot 10^{22}\,\mathrm{m}^{-3}$).

8. For the quantitative estimate of parameters characterizing the non-stationarity of homogenous nucleation process, additional experimental studies are required; yet, the volume densities of nanocrystals obtained through integration of equation (11) with reasonable (from physical point of view) parameters, indicates about a possibility of using the approximate Thurnbull–Fisher classical model to analyze the process of nano-phase composites formation.

Conflict of interest

The authors declare that they have no conflict of interest.

References

[1] A. Inoue, H. Kimura. Mater. Sci. Eng. A **286**, 1 (2000).
[2] H. Chen, Y. He, G.J. Shiflet, S.J. Poon. Scripta Met. Mater. **25**, *6*, 1421 (1991).
[3] P.A. Uzhakin, V.V. Tchirkova, N.A. Volkov, G.E. Abrosimova. FTT **66**, *1*, 8 (2024). (in Russian).
[4] U. Kester, U. Gerold. V sb.: Metallichasie styokla. Ionnaya struktura, elektronny perenos i kristallizatsiya / Eds. G. Bek, G. Gyunterodt, Mir, M. (1983). P. 325. (in Russian).
[5] D.R. Allen, J.C. Foley, J.H. Perepezko. Acta Mater. **46**, *2*, 431 (1998).
[6] K. Hono, Y. Zhang, A.P. Tsai, A. Inoue, T. Sakurai. Scripta Met. Mater. **32**, *2*, 191 (1995).
[7] M.T. Clavaguera-Mora, N. Clavaguera, D. Crespo, T. Pradell. Prog. Mater. Sci. **47**, 559 (2002).
[8] V.I. Tkatch, S.G. Rassolov, T.N. Moiseeva, V.V. Popov. J. Non-Cryst. Solids **351**, 1658 (2005).
[9] S.G. Rassolov, V.I. Tkatch, V.V. Maslov, V.V. Maksimov, K.A. Svyrydova, I.V. Zhikharev. Phys. Status Solidi C **7**, *5*, 1340 (2010).
[10] X.-L. Wang, J. Almer, C.T. Liu, Y.D. Wang, J.K. Zhao, A.D. Stoica, D.R. Haeffner, W.H. Wang. Phys. Rev. Lett. **91**, 256501 (2003).
[11] K. Sato, H. Murakami, W. Sprengel, H.-E. Schaefer, Y. Kobayashi. Appl. Phys. Lett. **94**, 171904 (2009).
[12] A.K. Gangopadhyay, T.K. Croat, K.F. Kelton. Acta Mater. **48**, 4035 (2000).
[13] K.K. Sahu, N.A. Mauro, L. Longstrech-Spoor, D. Saha, Z. Nussinov, M.K. Miller, K.F. Kelton. Acta Mater. **58**, 4199 (2010).
[14] H. Nitsche, F. Sommer, E.J. Mittemeijer. J. Non-Cryst. Solids **351**, 3760 (2005).
[15] J.H. Perepezko, S.D. Imhoff, R.J. Hebert. J. Alloys Compd. **495**, 360 (2010).
[16] T. Duan, Y. Shen, S.D. Imhoff, F. Yi, P.M. Voyles, J.H. Perepezko. J. Chem. Phys. **158**, 064504 (2023).
[17] S.G. Rassolov, V.I. Tkatch, V.V. Maksimov, O.V. Kovalenko, T.N. Moiseeva, V.V. Popov. Fizika i tekhnika vysokikh davleniy **23**, *1*, 18 (2013). (in Russian).
[18] J. Antonowicz. J. Non-Cryst. Solids **351**, 2383 (2005).
[19] J.S. Blazquez, M. Millan, C.F. Conde, A. Conde. J. Alloys Compd. **505**, 91 (2010).
[20] A. Inoue. Prog. Mater. Sci. **43**, 365 (1998).
[21] S.V. Vasiliev, A.I. Limanovskii, V.M. Tkachenko, T.V. Tsvetkov, K.A. Svyrydova, V.V. Burkhovetskii, V.N. Sayapin, O.A. Naumchuk, A.S. Aronin, V.I. Tkatch. Mater. Sci. Eng. A **850**, 143420 (2022).
[22] P. Wesseling, B.C. Ko, J.J. Lewandowski. Scripta Mater. **48**, 1537 (2003).
[23] H.W. Yang, J. Wen, M.X. Quan, J.Q. Wang. J. Non-Cryst. Solids **355**, 235 (2009).
[24] S.S. Gorelik, Yu.A. Skakov, L.N. Rastorguev. Rentgenograficheskiy i elektronno-opticheskiy analiz. MISIS, M., (2002). 360 p. (in Russian).
[25] J.O. Wang, H.W. Zhang, X.J. Gu, K. Lu, F. Sommer, E.J. Mittemeijer. Mater. Sci. Eng. A **375–377**, 980 (2004).
[26] J. Christian. Teoriya prevrashcheniy v metallakh i splavakh. Ch. 1. Mir, M. (1978). 806 p. (in Russian).
[27] K.F. Kelton. Solid State Phys.: Adv. Res. Appl. **45**, 75 (1991).

[28] V.P. Skripov, V.P. Koverda Spontannaya kristallizatsia pereokhlazhdennykh zhidkostei. Nauka, M. (1984). 232 p. (in Russian).
[29] D. Kashchiev. Surf. Sci. **14**, *1*, 209 (1969).
[30] A.V. Osipov. FTT **36**, *5*, 1213 (1994). (in Russian).
[31] V.V. Sleyozov, Yu.P. Shmeltser FTT **43**, *6*, 1101 (2001). (in Russian).
[32] V.V. Sleyozov, S.A. Kukushkin. FTT **38**, *2*, 433(1996). (in Russian).
[33] V.V. Sleyozov, P.N. Ostapchuk. FTT **53**, *3*, 544 (2011). (in Russian).
[34] R.C. Tolman. J. Chem. Phys. **17**, 333 (1949).
[35] P.V. Gordon, S.A. Kukushkin, A.V. Osipov. FTT **44**, *11*, 2079 (2002). (in Russian).
[36] S.A. Kukushkin, A.V. Osipov. Kinetika i kataliz **49**, *1*, 85 (2008). (in Russian).
[37] S.A. Kukushkin, A.V. Osipov. UFN, **168**, *10*, 1083 (1998). (in Russian).
[38] D. Turnbull, J.C. Fisher. J. Chem. Phys. **17**, *1*, 71 (1949).
[39] Svoistva elementov. Spravochnik / Pod. red. G.V. Samsonova. Ch. 1. Metallurgiya, M., (1980) 600 p. (in Russian).
[40] C.V. Thompson, F. Spaepen. Acta Metallurg. **22**, *12*, 1855 (1979).
[41] X. Ji, Y. Pan. J. Non-Cryst. Solids **353**, 2443 (2007).
[42] F. Spaepen. Solid State Phys.: Adv. Res. Appl. **47**, 1 (1994).
[43] L. Battezzati. Mater. Sci. Eng. A **304**–**306**, 103 (2001).
[44] J.W.P. Schmelzer, T.V. Tropin, V.M. Fokin, A.S. Abyzov, E.D. Zanotto. Entropy **22**, 1098 (2020).
[45] K.F. Kelton, T.K. Croat, A.K. Gangopadhyay, L.-Q. Xing, A.L. Greer, M. Weyland, X. Li, K. Rajan. J. Non-Cryst. Solids **317**, 71 (2003).
[46] X.Y. Jiang, Z.C. Zhong, A.L. Greer. Mater. Sci. Eng. A **226**–**228**, 789 (1997).
[47] C.V. Thompson, F. Spaepen. Acta Met. **31**, *12*, 2021 (1983).
[48] S.V. Vasiliev, V.I. Parfenii, A.S. Aronin, E.A. Pershina, V.I. Tkatch. J. Alloys Comp. **869**, 159285 (2021).

Translated by T.Zorina